Fluid Phase Equilibria 409 (2016) 408–416

Contents lists available at ScienceDirect

Fluid Phase Equilibria

journal homepage: www.elsevier.com/locate/fluid

# Modeling gas solubilities in imidazolium based ionic liquids with the [$Tf_2N$] anion using the GC-EoS

Selva Pereda [a, *], Sona Raeissi [b], Alfonsina E. Andreatta [c], Susana B. Bottini [a], Maaike Kroon [e], Cor J. Peters [d, e]

[a] Planta Piloto de Ingeniería Química, Universidad Nacional del Sur-CONICET, Camino La Carrindanga Km 7, CC 717, 8000 Bahía Blanca, Buenos Aires, Argentina
[b] School of Chemical and Petroleum Engineering, Shiraz University, Mollasadra Ave., Shiraz, 71345, Iran
[c] IDTQ Grupo vinculado PLAPIQUI-CONICET, Universidad Nacional de Cordoba X5016GCA, Av. Vélez Sarsfield, 1611 Córdoba, Argentina
[d] The Petroleum Institute, Chemical Engineering Department, P.O. Box 2533, Abu Dhabi, United Arab Emirates
[e] Eindhoven University of Technology, Department of Chemical Engineering and Chemistry, Separation Technology Group, Den Dolech 2, 5612 AZ Eindhoven, The Netherlands

ARTICLE INFO

*Article history:*
Received 31 August 2015
Received in revised form
9 October 2015
Accepted 21 October 2015
Available online 24 October 2015

*Keywords:*
GC-EoS
Group contribution
Equation of state
1-Alkyl-3-methylimidazolium bis(trifluoromethyl-sulfonyl)imide
1-Alkyl-3-methylimidazolium bis(trifluoromethyl-sulfonyl)amide
$CO_2$
CO
$H_2$
Alkane

ABSTRACT

The group contribution equation of state (GC-EoS) is extended to model gas solubilities in the homologous 1-alkyl-3-methylimidazolium bis(trifluoromethyl-sulfonyl) imide family. The gases considered in this work are $CO_2$, CO, $H_2$, $CH_4$, and $C_2H_6$. The model parameters were estimated on the basis of 1400 experimental data points in the temperature range of 278–460 K and pressures up to 160 bars. A correlation is also presented to calculate the critical diameter, a characteristic parameter of the GC-EoS repulsive term, as a function of the ionic liquid molar volume. Density data is most often available for ionic liquids; hence, the correlation provides a predictive method for ionic liquids not included in the parameterization process. The new parameters were then used to predict the phase behavior of binary mixtures containing different solutes (including $C_3H_8$, $C_4H_{10}$, and $C_6H_{14}$) and ionic liquids with different chain lengths than those used in the parameterization process.



## 1. Introduction

There are a number of industrial processes that call for an efficient technology for $CO_2$ recovery from gas streams: for example, the removal of acid gases from natural gas or biogas, the purification of the products of steam reforming, the water gas shift reaction and the integrated gasification cycle. Additionally, the growing concern about global warming and environmental pollution, are making governmental regulations on $CO_2$ emissions more stringent every day.

Currently, the available commercial $CO_2$ capture technologies include chemical and physical absorption, physical adsorption, membrane separation and cryogenic distillation. A number of authors have proposed, as an alternative method, the use of ionic liquid supported membranes for $CO_2$ separation [1,2]. Room temperature ionic liquids (RTILs or simply ILs) are liquid organic salts, having negligible vapor pressure and high solvation power. These characteristics make them good candidates to replace conventional organic solvents. Moreover, many ILs have high thermal stability. This property, together with the fact that they have almost no vapor pressure, minimize solvent losses in the gas stream and help to reduce the solvent make-up required in separation processes.

A thermodynamic model able to predict gas solubility in ionic liquids is required for the proper design and optimization of such processes. A literature review on the thermodynamic models

* Corresponding author.
*E-mail addresses:* spereda@plapiqui.edu.ar (S. Pereda), raeissi@shirazu.ac.ir (S. Raeissi), aandreatta@plapiqui.edu.ar (A.E. Andreatta), cpeters@pi.ac.ae (C.J. Peters).

http://dx.doi.org/10.1016/j.fluid.2015.10.037
0378-3812/

applied to ionic liquid mixtures, shows that various approaches have been investigated, mainly consisting of equations of state [3–9] and excess Gibbs energy models such as NRTL [10–12], UNIQUAC [12–14], and UNIFAC [15–17]. However, each method has its own advantages and shortcomings over the others. For example, the excess Gibbs energy models are not suitable for high-pressure conditions typical in gas processing, while the classic cubic equations of state face the limitation of the lack of experimental information on the critical properties of ionic liquids. Considering such shortcomings and the large variety of ionic liquids that may be available, group contribution methods appear to be an interesting alternative. The group contribution equation of state (GC-EoS) is an attractive model, taking into account that the information on the critical properties of pure compounds may not be required. Another advantage of using the GC-EoS is its ability to model phase equilibria in size-asymmetric mixtures [18–20]. GC-EoS uses the Carnahan-Starling [21] equation for hard spheres, which is a more realistic model for the repulsive contribution than the simple van der Waals repulsive term used by the majority of cubic equations of state. The combination of this repulsive term with a group contribution NRTL attractive term, makes the GC-EOS a promising tool to model the phase behavior of mixtures of gases and ionic liquids. Breure et al. [22] were the first to use the GC-EoS to model $CO_2$ solubility in ionic liquids. Bubble points were predicted for mixtures of $CO_2$ with the homologous families of 1-alkyl-3-methylimidazolium hexafluorophosphate and tetrafluoroborate. The agreement between experimental and predicted bubble points were excellent for pressures up to 20 MPa, even for pressures up to about 100 MPa. The results showed the capability of the GC-EOS to describe phase equilibria of such systems. Later, Bermejo et al. [23] used the GC-EoS to describe the phase behavior of different gases with ionic liquids of the methylimidazolium bis[(trifluoromethyl) sulfonyl]imide family. For most of the systems, the average deviations between experimental data and model predictions were below 10%. However, since at the time that the article was published, experimental data on the other members of the homologous family were yet unavailable, the authors concluded that further studies with the GC-EoS would be required to verify the applicability of the model to other members of the family.

In the present work, the GC-EOS is applied to model gas solubilities ($H_2$, $CO_2$, CO, $CH_4$, $C_2H_6$) in the various members of the homologous 1-alkyl-3-methylimidazolium bis(trifluoromethylsulfonyl)imide family (abbreviated as [$C_n$mim][$Tf_2$N]). Furthermore, liquid–liquid equilibria is also considered and modeled. The predictive capability of the equation is of particular significance in this work, since the critical diameter of the ionic liquid is not fitted to experimental data. It is predicted with a general correlation proposed in this work, as a function of the density of the pure ionic liquid, a property which is most often readily known for ionic liquids. In this way, our approach provides a predictive capacity, which widens the applicability of the model to different conditions and multiphase equilibria, as compared to the previous GC models for gas solubility in ionic liquids.

## 2. Thermodynamic model

The group contribution equation of state was proposed by Skjold-Jørgensen [24,25], for modeling particularly high-pressure equilibria. The model is based on the generalized van der Waals partition function, combined with the local composition principle and a group contribution approach. Based on extensive testing, the GC-EOS has proven to be a reliable method for phase equilibrium calculations for mixtures containing widely differing components.

The GC-EoS can be written as the sum of two different contributions to the residual Helmholtz energy:

$$A^{res} = A^{rep} + A^{att} \quad [1]$$

The Carnahan–Starling repulsive term follows the expression developed by Mansoori and Leland [26] for mixtures of hard spheres. It is a function of the critical hard sphere diameter, characteristic of the pure-compound molecular size, and has no binary or higher-order parameters. This free-volume contribution makes the model especially suited for predicting the effects of large molecular size differences on the excess properties of the mixture, as shown in several publications on the subject of supercritical fluid applications [27–31].

The attractive term is a group contribution version of the NRTL expression, with density-dependent mixing rules. The attractive energy between like groups is calculated from pure group parameters; binary parameters are introduced to quantify interactions between unlike groups. Details of the model are given in the Appendix.

When the GC-EOS model is applied to ILs, it is necessary to determine the functional groups that conform the molecules. Similar to UNIFAC, groups should be defined as neutral as possible. For this reason, the ionic core (cation + anion) is defined as the IL group, while the hydrocarbon chain is divided into the paraffinic groups $CH_3$ and $CH_2$ (see Fig. 1). This makes possible to describe the complete members of the [$C_n$mim][$Tf_2$N] family with only three functional groups, leading to an important reduction in the number of binary interaction parameters.

### 2.1. Parameterization of the repulsive term

The free volume term of the residual Helmholtz energy contains only one characteristic parameter, which is the critical hard sphere diameter (*dc*). There are three different ways to calculate *dc* for each compound: (i) direct calculation from the critical temperature and pressure (see Equation (A6) in the Appendix); (ii) optimization of *dc* by fitting a given point of the pure-component vapor pressure curve; (iii) computation of *dc* with a correlation for high molecular weight compounds proposed by Bottini et al. [18], based on the van der Waals molecular volume $r_i^{vdW}$:

$$\log(dc_i) = 0.4152 + 0.4128 \cdot \log\left(r_i^{vdW}\right) \quad [2]$$

In the case of permanent gases, the first procedure must be used. Ordinary solvents are generally modeled using method (ii), which usually gives *dc* values within 5% of those given by method (i). However, this difference is important, since pure component vapor pressures are quite sensitive to *dc* [25]. High molecular weight compounds present extremely low vapor pressures and their critical properties are usually unknown. For this reason, they require the use of method (iii). Ionic liquids also have negligible vapor pressures and unknown critical points. Bottini et al. [18] estimated $r_i^{vdW}$ using the Bondi [32] group contribution method. However, the latter method was developed for non-ionic organic compounds, so its use for ionic liquids would be inappropriate. In addition, several

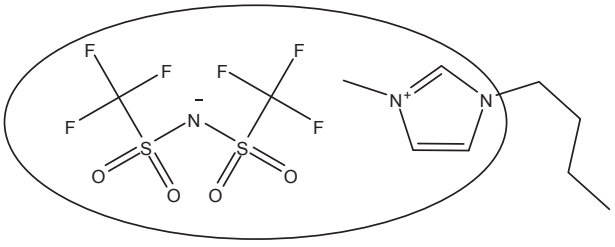


**Fig. 1.** Group definition for [-mim][$Tf_2$N].

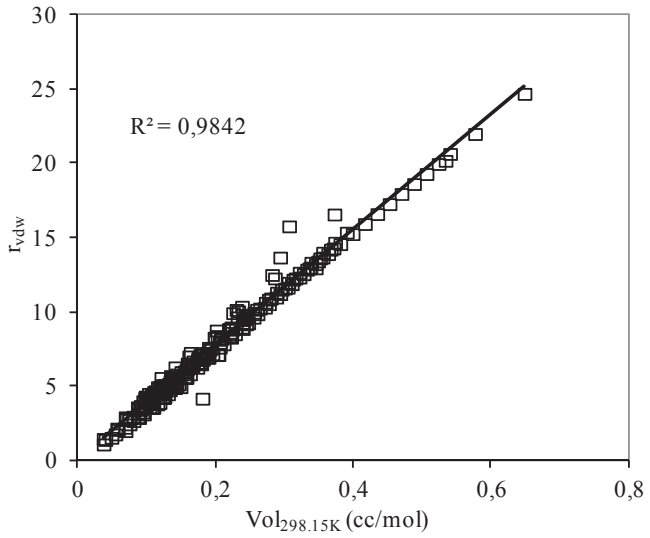


**Fig. 2.** Correlation between the van der Waals volume and the molar volume at 298 K, for 270 organic compounds; data taken from Ref. [34].

of the groups required for describing ionic liquids are not available.

The molar volume of the pure compound is an alternative source of information to estimate the van der Waals volume, as shown by Vera et al. [33]. The close correlation between the van der Waals volume and the molar volume at 298 K, is shown in Fig. 2 for a variety of 270 organic compounds [34], including hydrocarbons, alcohols, acids, amines, ethers, esters, aromatic and polyfunctional compounds.

The linear regression of the data shown in Fig. 2 resulted in the following equation:

$$r_i^{vdW} = 0.039 \cdot V_{298K}(cc/mol) \quad [3]$$

Table 1 shows that the deviation of this correlation, per family of organic compounds, is lower than 6% in every case, and 3.72% on average. Domanska and Mazurowska [13] were the first to apply Vera's approach to estimate $r^{vdW}$ for ionic liquids. These authors modeled the solubility of 1,3-dialkylimidazolium chloride, hexafluorophosphate, and methylsulfonate in organic solvents with UNIQUAC and NRTL. They reported a value of 0.029281 for the proportionality constant in Equation (3). The original value proposed by Vera for this constant was 0.036, based on molar volumes at 293 K. The small difference with the proportionality constant determined in this work is due to the slight temperature difference in the molar volume.

**Table 1**
Average absolute relative deviation, per family of organic compounds, between $r^{vdW}$ reported in DIPPR [34] and that calculated by Equation (3).

| Organic family | AARD (%) |
|---|---|
| n-Alkane | 3.37 |
| 1-Alkene | 4.13 |
| Cycloalkanes | 2.55 |
| Alkil-benzene | 1.99 |
| Polyaromatic | 5.08 |
| 1-Alkanols | 1.20 |
| Aromatic alcohol | 4.25 |
| Amines | 3.41 |
| Aromatic amines | 5.30 |
| Carboxilic acids | 0.86 |
| Esters | 5.13 |
| Ethers | 5.90 |
| Ketones | 4.00 |
| Polyfunctional | 4.90 |
| All families | 3.72 |

**Table 2**
Molecular weight, molar volume at 298 K, van der Waals volume, and GC-EoS critical diameter for the ionic liquids of the [$C_n$mim][$Tf_2$N] family.

| Ionic liquid | Mw/g mol$^{-1}$ | V/cc mol$^{-1}$[a] | $r^{vdW}$ | $dc$/cm mol$^{-1/3}$ |
|---|---|---|---|---|
| [$C_2$mim][$Tf_2$N] | 391.31 | 258.6 | 10.35 | 6.825 |
| [$C_3$mim][$Tf_2$N] | 405.34 | 275.4 | 11.02 | 7.005 |
| [$C_4$mim][$Tf_2$N] | 419.36 | 292.3 | 11.69 | 7.178 |
| [$C_5$mim][$Tf_2$N] | 433.39 | 309.1 | 12.37 | 7.346 |
| [$C_6$mim][$Tf_2$N] | 447.42 | 325.9 | 13.04 | 7.509 |
| [$C_8$mim][$Tf_2$N] | 475.48 | 359.6 | 14.39 | 7.820 |

[a] Molar volume calculated with the correlation of Gardas et al. [35].

**Table 3**
Activity coefficient at infinity dilution of n-alkanes ($C_5$ to $C_{12}$) in various ILs: Experimental data source and deviations.

| Binary system | $T$/K | $P$/MPa | $\gamma^\infty$ | Source | $N$ | AAD% for $\gamma^\infty$ |
|---|---|---|---|---|---|---|
| [$C_1$mim][$Tf_2$N] | 303–333 | 0.1 | 18.9–66.3 | [52] | 12 | 1.89 |
| [$C_2$mim][$Tf_2$N] | 293–345 | 0.1 | 15.4–151.2 | [52,53] [a] | 32 | 4.90 |
| [$C_4$mim][$Tf_2$N] | 293–355 | 0.1 | 7.95–102.86 | [52,54] | 46 | 4.75 |
| [$C_6$mim][$Tf_2$N] | 298–343 | 0.1 | 4.1–15.1 | [55,56] | 36 | 7.36[b] |

[a] The data of [57] was not included in the parameter fitting because they are in disagreement with the other two references available.
[b] Some experimental data points at the same temperature are in disagreement among [55] and [56].

Table 2 summarizes the $dc$ values for all of the ionic liquids investigated in this study, calculated with Equations (2) and (3).

The critical diameter is used to calculate the temperature-dependent hard sphere diameter, which is also a function of the critical temperature (see Equation (A5) in the Appendix). This temperature dependence was empirically determined by fitting vapor pressures of pure organic compounds to the Carnahan-Starling equation, combined with the attractive term of the Soave-Redlich-Kwong (SRK) equation [24]. In this work, a constant value of critical temperature (1000 K) is used for all ionic liquids.

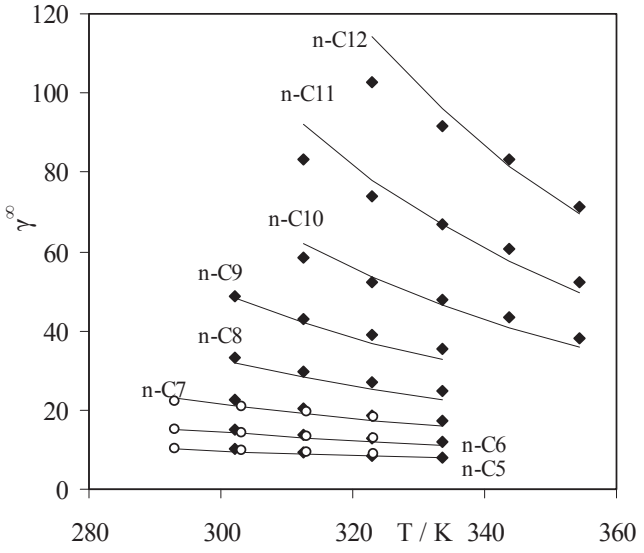


**Fig. 3.** Activity coefficient at infinite dilution of n-alkanes in [$C_4$mim][$Tf_2$N]. GC-EoS (—). Experimental data: ○ [52] and ◆ [54].

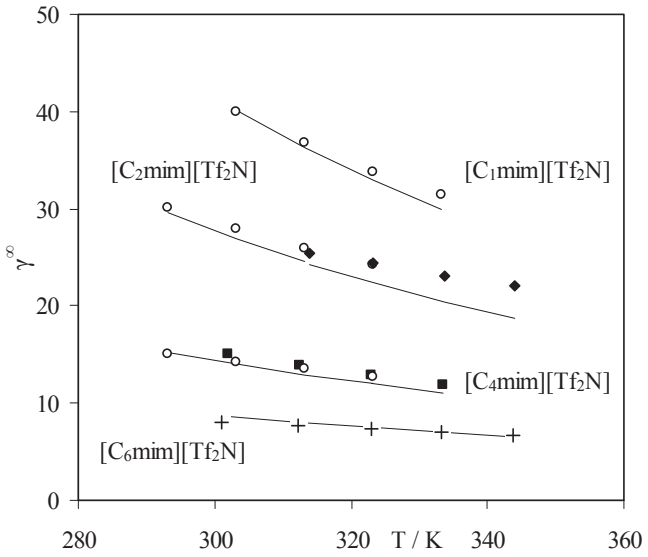


**Fig. 4.** Activity coefficient at infinite dilution of n-hexane in various ionic liquids. GC-EoS (—)Experimental data: ○ [52], ◆ [53], ■ [54], + [55].

### 2.2. Parameterization of the attractive term

The attractive term of the GC-EoS considers that energy interactions take place through the surfaces of characteristic groups, rather than through the surfaces of the parent molecules [25]. Each functional group is characterized by a surface area $q$ (analogous to the one used in the UNIFAC model) and a reference temperature $T^*$ (set equal to 600 K for most functional groups). Following a group-contribution approach, the normalized van der Waals area of a compound $i$ can be calculated as the sum of the constituent group area parameters, $q_j$:

$$q_i = \sum_j \nu_j^i \cdot q_j \quad [4]$$

where $\nu_j^i$ is the number of groups $j$ in molecule $i$.

The group surface area in the GC-EoS is normally calculated using the Bondi [32] group contribution method. Similarly to volume, this method is not readily applicable to ionic liquids. Nevertheless, the surface area of the ionic core [-mim][$Tf_2N$] can be computed by subtracting the area of the paraffinic chain, which is well known, from the area of the parent IL molecule. The surface area of the IL molecule can be calculated through Equation (5) [36]:

$$q_i = \frac{(z-2)\cdot r_i^{vdW}}{z} + \frac{2\cdot(1-l_i)}{z} \quad [5]$$

where $r_i^{vdW}$ is the van der Waals volume, $z$ the coordination number (set equal to 10), and $l_i$ the bulk factor. The selection of $l_i = 0$ results in $q_i$ values for ionic liquids comparable to those computed by Banerjee et al. [14] via the Polarizable Continuum Model.

The attractive term also requires information on binary interaction parameters between unlike functional groups. It is important to highlight that only the interaction parameters involving the new group ([-mim][$Tf_2N$]) are fitted in this work to literature data [37–51]. The parameters for the previously available groups were taken from Skold-Jørgensen [25].

## 3. Results and discussion

The first parameters to be fitted were the pure group [-mim][$Tf_2N$] surface energy parameter and the binary energy interactions

**Table 4**
Binary equilibrium database and GC-EoS correlation. Δx% and ΔT% are the percent average relative deviation[b] in composition and temperature, respectively.

| Binary system | Mole fraction | T/K | P/MPa | Source | N | Δx% | ΔT% |
|---|---|---|---|---|---|---|---|
| $CO_2$ + | | | | | | | |
| [$C_2$mim][$Tf_2N$] | 0.085–0.585 | 313–450 | 0.422–14.10 | [37] | 98 | 2.52 | 1.33 |
| [$C_4$mim][$Tf_2N$] | 0.123–0.593 | 312–450 | 0.626–14.40 | [40] | 86 | 2.24 | 1.26 |
| [$C_4$mim][$Tf_2N$] | 0.092–0.512 | 279–340 | 0.29–4.80 | [38] | 16 | 4.30 | [a] |
| [$C_4$mim][$Tf_2N$] | 0.176–0.752 | 298–333 | 1.13–13.24 | [39] | 55 | 2.99 | [a] |
| [$C_6$mim][$Tf_2N$] | 0.142–0.648 | 278–369 | 0.422–13.82 | [42] | 75 | 2.56 | 1.44 |
| [$C_6$mim][$Tf_2N$] | 0.199–0.758 | 298–333 | 1.31–11.56 | [39] | 28 | 2.97 | [a] |
| [$C_6$mim][$Tf_2N$] | 0.099–0.676 | 293–413 | 0.60–9.91 | [41] | 25 | 4.25 | [a] |
| [$C_8$mim][$Tf_2N$] | 0.246–0.791 | 298–333 | 1.36–11.47 | [39] | 22 | 3.41 | [a] |
| CO + | | | | | | | |
| [$C_4$mim][$Tf_2N$] | 0.051–0.099 | 310–458 | 4.79–10.34 | [43] | 46 | 2.63 | 4.07 |
| [$C_6$mim][$Tf_2N$] | 0.052–0.125 | 300–438 | 4.05–11.67 | [44] | 45 | 2.25 | 3.37 |
| $H_2$ + | | | | | | | |
| [$C_2$mim][$Tf_2N$] | 0.037–0.066 | 313–453 | 5.68–14.33 | [45] | 53 | 1.56 | 1.04 |
| [$C_4$mim][$Tf_2N$] | 0.021–0.108 | 313–450 | 2.69–15.43 | [46] | 57 | 2.99 | 2.08 |
| [$C_6$mim][$Tf_2N$] | 0.033–0.061 | 300–369 | 4.58–11.85 | [48] | 67 | 4.52 | 3.18 |
| [$C_6$mim][$Tf_2N$] | 0.007–0.074 | 293–413 | 1.47–9.82 | [47] | 25 | 7.05 | [a] |
| $CH_4$ + | | | | | | | |
| [$C_4$mim][$Tf_2N$] | 0.030–0.225 | 300–450 | 1.51–16.10 | [49] | 39 | 4.02 | 5.04 |
| [$C_6$mim][$Tf_2N$] | 0.089–0.093 | 293–413 | 0.06–0.51 | [50] | 24 | 1.60 | [a] |
| $C_2H_6$ + | | | | | | | |
| [$C_6$mim][$Tf_2N$] | 0.05–0.40 | 293–369 | 0.39–13.07 | [51] | 70 | 0.83 | 0.48 |
| $C_3H_8$ + | | | | | | | |
| [$C_6$mim][$Tf_2N$] | 0.016–0.19 | 280–340 | 0.87–10.5 | [38] | 14 | 6.78 | [a] |
| $C_4H_{10}$ + | | | | | | | |
| [$C_6$mim][$Tf_2N$] | 0.025–0.14 | 280–340 | 0.33–3.00 | [38] | 16 | 9.13 | [a] |
| $C_6H_{14}$ | | | | | | | |
| [$C_2$mim][Tf2N] | 0.008–0.08 | 353.15 | 0.18–1.4 | [5] | 10 | 2.63 | [a] |
| [$C_6$mim][Tf2N] | 0.011–0.19 | 353.15 | 0.094–1.13 | [17] | 12 | 2.08 | [a] |
| [$C_8$mim][Tf2N] | 0.015–0.30 | 353.15 | 0.093–1.38 | [17] | 13 | 2.06 | [a] |

[a] Isothermal data.
[b] $\Delta Z\% = \frac{1}{N}\sum_i^N \left|\frac{Z_{exp,i} - Z_{calc,i}}{Z_{exp,i}}\right|$

**Table 5**
GC-EoS pure group parameters.

| Group | $g_{ii}^*$/atm cm$^6$ mol$^{-2}$ | $g_{ii}'$ | $g_{ii}''$ | T*/K | q | Reference |
|---|---|---|---|---|---|---|
| $CH_3$ | 316910 | −0.9274 | 0 | 600 | 0.848 | [25] |
| $CH_2$ | 316910 | −0.9274 | 0 | 600 | 0.54 | [25] |
| [-mim][$Tf_2N$] | 501325 | −0.9006 | 0 | 600 | 7.098 | This work |
| $H_2$ | 179460 | −0.0843 | 0.1351 | 33.20 | 0.5710 | [25] |
| $CO_2$ | 531890 | −0.5780 | 0 | 304.2 | 1.261 | [25] |
| CO | 309610 | −0.1288 | −0.1074 | 132.9 | 1.060 | [25] |
| $CH_4$ | 402440 | −0.2762 | 0.0221 | 190.6 | 1.160 | [25] |
| $C_2H_6$ | 452560 | −0.3758 | 0 | 305.32 | 1.696 | [25] |

**Table 6**
GC-EoS binary energy interaction parameters.

| *i* | *j* | *kij* | *kij'* | *αij* | *αji* | Reference |
|---|---|---|---|---|---|---|
| $CH_3$ | $CH_2$ | 1.0 | 0 | 0 | 0 | [25] |
| | $H_2$ | 1.0630 | 0 | −1.0 | −1.0 | [25] |
| | $CO_2$ | 0.892 | 0 | 3.369 | 3.369 | [25] |
| | CO | 0.958 | −0.252 | −2.889 | −2.890 | [25] |
| | $CH_4$ | 0.998 | −0.061 | 0 | 0 | [25] |
| | $C_2H_6$ | 0.987 | 0 | 0 | 0 | [25] |
| | [-mim][$Tf_2N$] | 0.7238 | 0 | 1.7185 | 4.050 | This work |
| $CH_2$ | $H_2$ | 1.216 | 0 | −1. | −1. | [25] |
| | $CO_2$ | 0.814 | 0 | 3.369 | 3.369 | [25] |
| | CO | 0.958 | −0.252 | −2.889 | −2.890 | [25] |
| | $CH_4$ | 0.940 | 0.056 | 0 | 0 | [25] |
| | $C_2H_6$ | 0.987 | 0 | 0 | 0 | [25] |
| | [-mim][$Tf_2N$] | 0.7656 | 0 | 1.7185 | 4.050 | This work |
| [-mim][$Tf_2N$] | $H_2$ | 1.0300 | 0.200 | 0 | 0 | This work |
| | $CO_2$ | 0.8839 | 0 | 5.729 | 4.400 | This work |
| | CO | 0.7496 | −0.163 | 0.8504 | 0.8504 | This work |
| | $CH_4$ | 0.800 | −0.200 | 0 | 0 | This work |
| | $C_2H_6$ | 0.7579 | −0.186 | 0 | 0 | This work |

between the [-mim][$Tf_2N$] group and the paraffinic groups, $CH_2$ and $CH_3$. For this purpose, experimental data on infinite dilution activity coefficients of n-alkanes in different ionic liquids was used, as given in Table 3. This correlation process allowed fitting the IL parameters, without having to introduce new functional groups other than those present in the ionic liquid molecule. Fig. 3 shows, for example, the GC-EoS correlation of activity coefficients at infinite dilution for various members of the n-alkane family in [$C_4$mim][$Tf_2N$], while Fig. 4 presents the correlated infinite dilution activity coefficients of n-hexane in the different ionic liquids investigated in this work. The relative deviations between the results of the GC-EoS calculations and the experimental activity coefficients, also given in Table 3, indicate that a good correlation was achieved.

In the next step, the experimental data on the solubilities of the different gases under study, as given in Table 4, were used to fit the binary energy interaction parameters between each gas and the new IL group. During this procedure, the predictive capacity of the model was also checked by adjusting only several isopleths of a certain binary (gas + IL), and predicting not only the remaining isopleths of that binary, but also the solubility of the same gas in other ILs with different alkyl chain lengths. This test is a challenge for the free-volume contribution term, because the model should be able to predict the behavior of components of different sizes, using the same unique set of parameters of the attractive term. In general, solubilities were predicted with errors below 5%. It is important to highlight that the size of the IL was not fitted to experimental data, but computed via density information alone. At the end of the parameterization process, all consistent data available were included in the optimization, in order to get the best final set of parameters. The resulting parameters are reported in Tables 5 and 6. The model performance is shown for each gas in Figs. 5–9.

Fig. 10 shows the solubility of each studied gas in [$C_6$mim][$Tf_2N$]

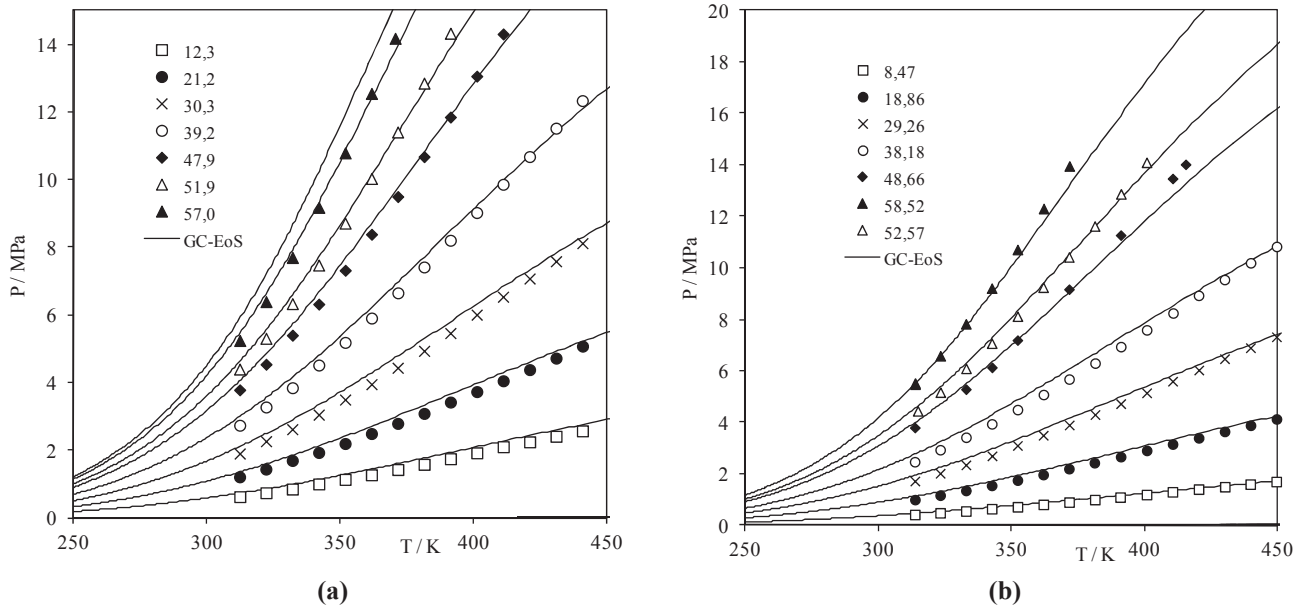


**Fig. 5.** Carbon dioxide solubility in: (a) [$C_2$mim][$Tf_2N$]. Experimental data [37]: (b) [$C_4$mim][$Tf_2N$]. Experimental data: [40].

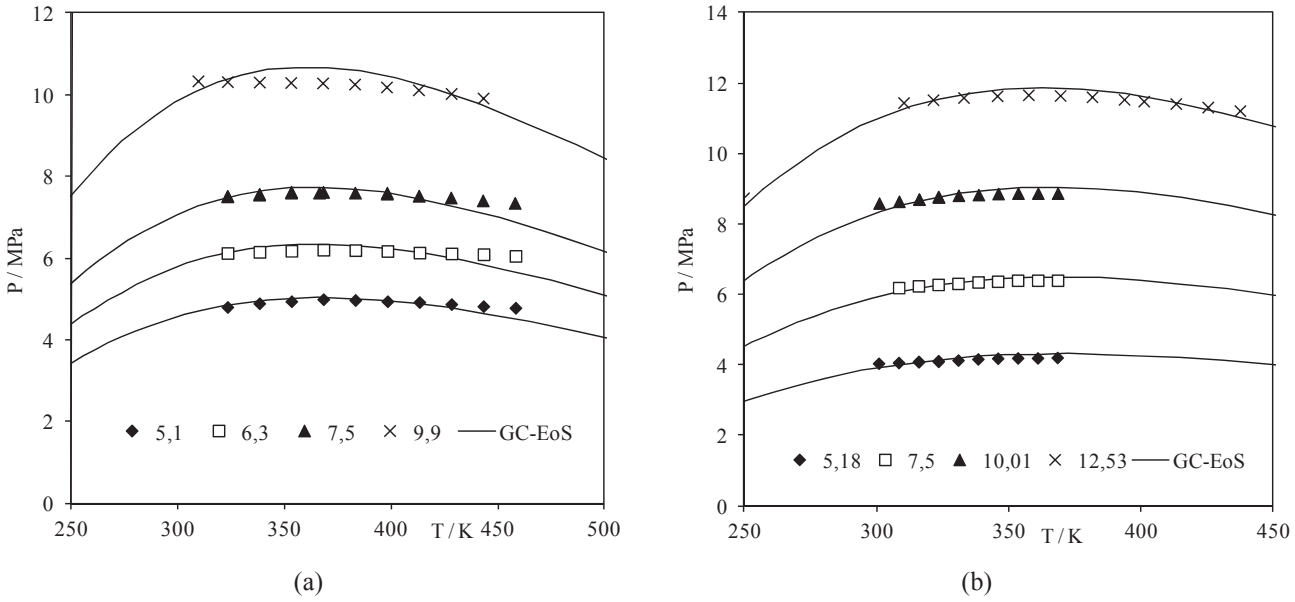


**Fig. 6.** Carbon monoxide solubility in: (a) [$C_4$mim][$Tf_2$N]. Experimental data: [43]; (b) [$C_6$mim][$Tf_2$N]. Experimental data [44].

at 293–353 K, in a pressure-composition diagram. As can be seen, GC-EoS predicts with high accuracy not only the solubility of each gas, but also the liquid–liquid split shown by ethane at the lower temperature. Actually, GC-EoS is able to predict the LLE of higher molecular weight paraffins, as can be inferred by the model accuracy to correlate the activity coefficients of these compounds in the [$C_n$mim][$Tf_2$N] homologous family.

The results of the phase boundary calculations using these parameters are also summarized in Table 4 in the form of average relative deviations in concentration and temperature, and graphically in Figs. 5–10. The temperature dependence of the solubility of the various gases shows different behavior. The carbon dioxide and ethane solubility decreases with temperature, hydrogen increases, carbon monoxide stays more or less constant, while methane is constant at low pressures and decreases at higher pressures. In monovariant equilibria (one degree of freedom), the slope of the pressure vs. temperature curve is given by the Clapeyron equation [58]. In the case of the bubble point curve, this slope is given by $\partial P/\partial T = \Delta H/T \cdot \Delta V$, where $\Delta H$ is the enthalpy change of gas dissolution and $\Delta V$ is the volume change of gas dissolution. Therefore, at a given temperature, the slope of the pressure vs. temperature curve depends on the ratio between enthalpy and volume change of dissolution. This slope can have positive or negative values depending on the system components and the operating conditions. The thermodynamic basis and reasoning of the differing *P-T* solubility slopes of the various gases in ionic liquids has been explained in detail earlier [46] from several different perspectives, including the Scott-van Konynenburg phase transitions, Le

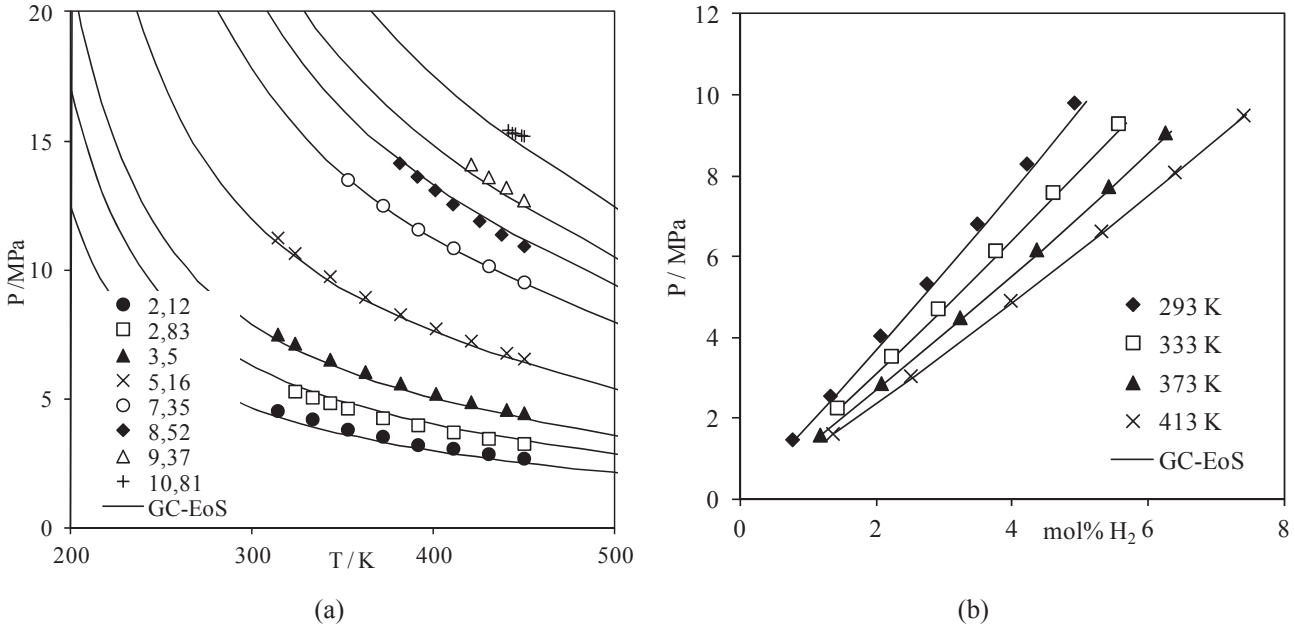


**Fig. 7.** Hydrogen solubility in (a) [$C_4$mim][$Tf_2$N]. Experimental data: [46]; (b) [$C_6$mim][$Tf_2$N]. Experimental data [47].

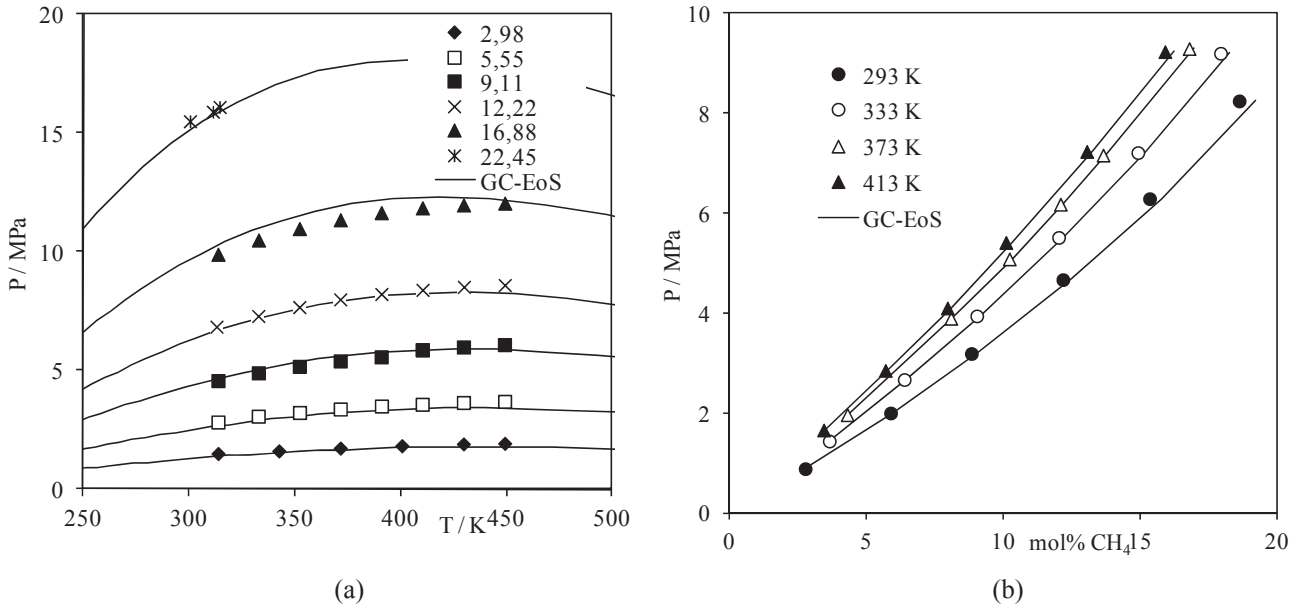


**Fig. 8.** Methane solubility in: (a) [$C_4$mim][$Tf_2$N]. Experimental data: [49]; and (b) [$C_6$mim][$Tf_2$N]. Experimental data [50].

Chatelier's principle, the Joule-Thompson effect, and the Lennard-Jones potential.

The errors in the calculated equilibrium concentrations and temperatures, as well as the closely matching trends in Figs. 5–10, indicate that the GC-EoS, with the group parameters obtained in this study, is accurate and capable of predicting the phase behavior of mixtures of gases with the [-mim][$Tf_2$N] ionic liquid family.

## 4. Conclusions

The group contribution equation of state has been extended for modeling gas solubility in the homologous 1-alkyl-3-methylimidazolium bis(trifluoro-methyl-sulfonyl)imide family. The free-volume or repulsive contribution to the GC-EoS Helmholtz energy is a function of the molecular critical diameter. A new procedure for computing this parameter for ionic liquids is proposed, which does not involve fitting experimental data. Therefore, it provides a global predictive approach. This procedure was demonstrated to work well, in each case where the model predictive capability was tested.

Regarding the attractive contribution of the Helmholtz energy, the model requires binary energy interaction parameters and the van der Waals surface ($q$) of the new [-mim][$Tf_2$N] group. The former are optimized to experimental data, while $q$ is computed from the molecular critical diameter. The resulting parameters give accurate phase equilibrium predictions with the GC-EoS. Not only

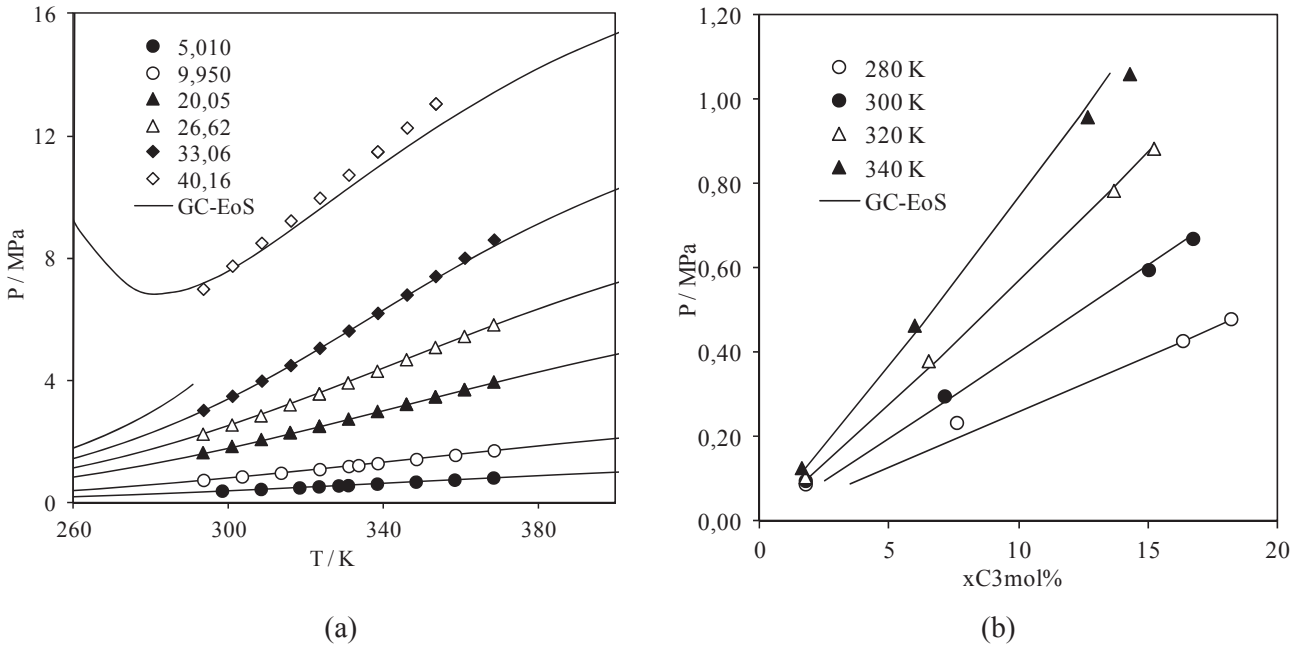


**Fig. 9.** (a) Ethane solubility in [$C_6$mim][$Tf_2$N]. Experimental data [51]; (b) Propane solubility in [$C_6$mim][$Tf_2$N]. Experimental data [38].

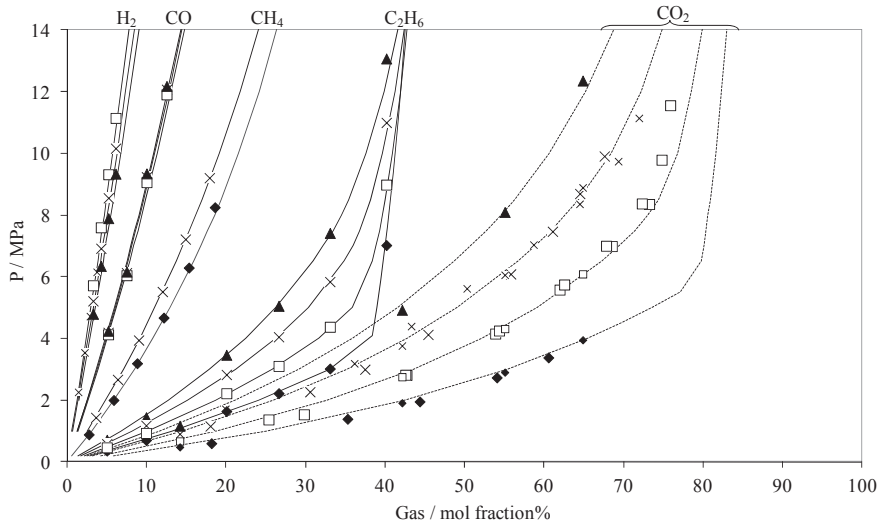


**Fig. 10.** Pressure-composition phase diagram for $H_2$, CO, $CH_4$, $C_2H_6$ and $CO_2$ with [$C_6$mim][$Tf_2$N] at 293 K ( ◆ ), 313 K( □ ), 333 K( × ) and 353 K( ▲ ). GC-EoS (— and —). Experimental data: $CO_2$ [39,41,42], CO [44], $H_2$ [47,48], $CH_4$ [50],and $C_2H_6$ [51].

vapor–liquid equilibrium calculations were performed successfully, but the extension of the method to predict liquid–liquid phase boundaries was also successful. Therefore, the equation is suitable for modeling such highly non-ideal systems.

## Acknowledgments

S. Pereda, A. Andreatta and S.B. Bottini acknowledge the financial support granted by the Consejo Nacional de Investigaciones Científicas y Técnicas (CONICET) and Universidad Nacional del Sur (UNS). S. Raeissi is grateful to Shiraz University and Technical University of Eindhoven for facilitating this collaboration.

## Appendix

There are two contributions to the residual Helmholtz function ($A^{res}$) in the GC-EoS model: the free volume ($A^{fv}$) and the attractive ($A^{att}$) terms.

$$A^{res} = A^{fv} + A^{att} \tag{A1}$$

The free volume contribution is represented by the extended Carnahan-Starling equation for mixtures of hard spheres developed by Mansoori and Leland [26].

$$(A/RT)^{fv} = 3(\lambda_1\lambda_2/\lambda_3)(Y-1) + \left(\lambda_2^3/\lambda_3^2\right)\left(-Y + Y^2 - \ln Y\right) + n\ln Y \tag{A2}$$

with:

$$Y = \left(1 - \frac{\pi\lambda_3}{6V}\right)^{-1} \tag{A3}$$

and

$$\lambda_k = \sum_i^{NC} n_i d_i^k \tag{A4}$$

$n_i$ being the number of moles of component $i$, $NC$ the number of components in the mixture, $n$ the total number of moles, $V$ the total volume and $d_i$ the hard-sphere diameter per mol of species $i$.

The following generalized expression gives the temperature dependence of the hard-sphere diameter:

$$d_i = 1.065655\, d_{ci}\{1 - 0.12\exp[-2T_{ci}/(3T)]\} \tag{A5}$$

where $d_{ci}$ and $T_{ci}$ are, respectively, the critical hard-sphere diameter and critical temperature of component $i$. The value of $d_{ci}$ can be determined from the critical properties:

$$d_{ci} = (0.08943RT_{ci}/P_{ci})^{1/3} \tag{A6}$$

Alternatively, it can be calculated by fitting to data on the vapor pressure of species $i$ [24]. For high molecular weight compounds (for which $T_c$ and $P_c$ are unknown and vapor pressure data is unavailable) the $d_{ci}$ value can be determined by fitting to experimental data on infinite dilution activity coefficients of mixtures of alkanes in the ionic liquid $i$ [18].

The attractive contribution to the Helmholtz energy accounts for dispersive forces between functional groups through a density-dependent, local-composition expression based on the NRTL model [59]:

$$(A/RT)^{att} = -\frac{z}{2}\sum_i^{NC} n_i \sum_j^{NG} \nu_j^i q_j \sum_k^{NG}\left(\theta_k g_{kj}\tilde{q}\tau_{kj}/RTV\right) \Big/ \sum_l^{NG}\theta_l\tau_{lj} \tag{A7}$$

with:

$$\tilde{q} = \sum_i^{NC} n_i \sum_j^{NG} \nu_j^i q_j \tag{A8}$$

$$\theta_j = \left(q_j/\tilde{q}\right)\sum_i^{NC} n_i \nu_j^i \tag{A9}$$

$$\tau_{ij} = \exp\left(\alpha_{ij}\Delta_{ij}\tilde{q}/RTV\right) \tag{A10}$$

$$\Delta g_{ij} = g_{ij} - g_{jj} \tag{A11}$$

$z$ being the coordination number (set equal to 10), $\nu_j^i$ the number

of groups of type $j$ in molecule $i$, $q_j$ the number of surface segments assigned to group $j$, $\widetilde{q}$ the total number of surface segments, $\theta_k$ the surface fraction of group $k$, $g_{ij}$ the attractive energy between segments of groups $i$ and $j$, and $\alpha_{ij}$ the non-randomness parameter.

The attractive energy, $g_{ij}$, is calculated from the energy between like-group segments through the following combination rule:

$$g_{ij} = k_{ij}\left(g_{ii}g_{jj}\right)^{1/2} \tag{A12}$$

where the binary interaction parameter $k_{ij}$ is symmetrical ($k_{ij} = k_{ji}$). Both, the attractive energy between like segments and the binary interaction parameter are temperature-dependent:

$$g_{jj} = g_{jj}^{*}\left(1 + g_{jj}'\left(T/T_j^{*} - 1\right) + g_{jj}'' \ln\left(T/T_j^{*}\right)\right) \tag{A13}$$

$$k_{ij} = k_{ij}^{*}\left\{1 + k_{ij}' \ln\left[2T/\left(T_i^{*} + T_j^{*}\right)\right]\right\} \tag{A14}$$

where $T_i^{*}$ is an arbitrary, but fixed, reference temperature for group $i$; $g_{jj}^{*}$, $g_{jj}'$ and $g_{jj}''$ are pure-group energy parameters, and $k_{ij}^{*}$ and $k_{ij}'$ are binary group interaction parameters.

## References


[1] P. Scovazzo, J. Kieft, D.A. Finan, C. Koval, D. DuBois, R. Noble, J. Mem. Sci. 238 (2004) 57–63.
[2] S. Raeissi, C.J. Peters, Green Chem. 11 (2009) 185–192.
[3] A. Shariati, C.J. Peters, J. Supercrit. Fluids 25 (2003) 109–117.
[4] R. Haghbakhsh, H. Soleymani, S. Raeissi, J. Supercrit. Fluids 77 (2013) 158–166.
[5] R. Kato, M. Krummen, J. Gmehling, Fluid Phase Equilibria 224 (2004) 47–54.
[6] M.T.M. Martinez, M.C. Kroon, C.J. Peters, J. Supercrit. Fluids 101 (2015) 54–62.
[7] F. Llovell, R.M. Marcos, N. MacDowell, L.F. Vega, J. Phys. Chem. B 116 (2012) 7709–7718.
[8] S.S. Ashrafmansouri, S. Raeissi, J. Supercrit. Fluids 63 (2012) 81–91.
[9] X. Ji, C. Held, G. Sadowski, Fluid Phase Equilib. 363 (2014) 59–65.
[10] T.V. Vasiltsova, S.P. Verevkin, E. Bich, A. Heintz, R. Bogel-Lukasik, U. Domanska, J. Chem. Eng. Data 50 (2005) 142–148.
[11] J.M. Crosthwaite, M.J. Muldoon, S.N.V.K. Aki, E.J. Maginn, J.F. Brennecke, J. Phys. Chem. B 110 (2006) 9354–9361.
[12] M. Döker, J. Gmehling, Fluid Phase Equilib. 227 (2005) 255–266.
[13] U. Domanska, L. Mazurowska, Fluid Phase Equilib. 221 (2004) 73–82.
[14] T. Banerjee, M.K. Singh, R.K. Sahoo, A. Khanna, Fluid Phase Equilib. 234 (2005) 64–76.
[15] R. Kato, J. Gmehling, J. Chem. Thermodyn. 37 (2005) 603–619.
[16] J. Wang, W. Sun, C. Li, Z. Wang, Fluid Phase Equilib. 264 (2008) 235–241.
[17] S. Nebig, R. Bölts, J. Gmehling, Fluid Phase Equilib. 258 (2007) 168–178.
[18] S.B. Bottini, T. Fornari, E.A. Brignole, Fluid Phase Equilib. 158–160 (1999) 211–218.
[19] S. Pereda, L. Rovetto, S.B. Bottini, J. Am. Oil Chem. Soc. 83 (2006) 461–467.
[20] S. Espinosa, G.M. Foco, A. Bermúdez, T. Fornari, Fluid Phase Equilib. 172 (2000) 129–143.
[21] N.F. Carnahan, K.E. Starling, J. Chem. Phys. 51 (1969) 635–636.
[22] B. Breure, S.B. Bottini, G.J. Witkamp, C.J. Peters, J. Phys. Chem. B 111–51 (2007) 14265–14270.
[23] M.D. Bermejo, D. Méndez, Á. Martín, Ind. Eng. Chem. Res. 49 (2010) 4966–4973.
[24] S. Skjold-Jørgensen, Fluid Phase Equilib. 16 (1984) 317–351.
[25] S. Skjold-Jørgensen, Ind. Eng. Chem. Res. 27 (1988) 110–118.
[26] G.A. Mansoori, J. Leland, J. Chem. Soc. Faraday Trans. 2 (68) (1972) 320–344.
[27] E.A. Brignole, S. Skjold-Jørgensen, A.A. Fredenslund, in: M. Radosz, M.A. Mc Hugh, V.J. Krukonis (Eds.), Application of the Group Contribution Equation of State to Supercritical Fluid Extraction in Supercritical Fluid Technology, Elsevier, Amsterdam, 1985, pp. 87–106.
[28] S. Pereda, S.B. Bottini, E.A. Brignole, AIChE J. 48–11 (2002) 2635–2645.
[29] S. Diaz, S. Espinosa, E.A. Brignole, J. Supercrit. Fluids 35 (2005) 49–61.
[30] S. Espinosa, S. Raeissi, E.A. Brignole, C.J. Peters, J. Supercrit. Fluids 32 (2004) 63–71.
[31] S. Diaz, H. Gros, E.A. Brignole, Comput. Chem. Eng. 24 (2004) 2069–2080.
[32] A. Bondi, Physical Properties of Molecular Crystals, Liquids and Glasses, Wiley, New York, 1968.
[33] J.H. Vera, S.G. Sayegh, G.A. Ratcliff, Fluid Phase Equilib. 1 (1977) 113–135.
[34] DIPPR801-Database, Thermophysical Properties Database, 1998.
[35] R.L. Gardas, H.F. Costa, M.G. Freire, P.J. Carvalho, I.M. Marrucho, I.M.A. Fonseca, A.G.M. Ferreira, J.A.P. Coutinho, J. Chem. Eng. Data 53 (2008) 805–811.
[36] D.S. Abrams, J.M. Prausnitz, AIChE J. 21 (1975) 116–128.
[37] A.M. Schilderman, S. Raeissi, C.J. Peters, Fluid Phase Equilib. 260 (2007) 19–22.
[38] B.C. Lee, S.L. Outcalt, J. Chem. Eng. Data 51 (2006) 892–897.
[39] S.N.V.K. Aki, B.R. Mellein, E.M. Saurer, J.F. Brennecke, J. Phys. Chem. B 108–52 (2004) 20355–20365.
[40] S. Raeissi, C.J. Peters, J. Chem. Eng. Data 54 (2009) 382–386.
[41] J. Kumełan, A. Pérez-Salado Kamps, D. Tuma, G. Maurer, J. Chem. Thermodyn. 38–11 (2006) 1396–1401.
[42] S. Raeissi, L. Florusse, C.J. Peters, J. Supercrit. Fluids 55 (2010) 825–832.
[43] S. Raeissi, L.J. Florusse, C.J. Peters, AIChE J. 59-10 (2013) 3886–3891.
[44] L.J. Florusse, S. Raeissi, C.J. Peters, J. Chem. Eng. Data 56 (2011) 4797–4799.
[45] S. Raeissi, A.M. Schilderman, C.J. Peters, J. Supercrit. Fluids 73 (2013) 126–129.
[46] S. Raeissi, C.J. Peters, AIChE J. 58-11 (2012) 3553–3559.
[47] J. Kumełan, A. Pérez-Salado Kamps, D. Tuma, G. Maurer, J. Chem. Eng. Data 51 (2006) 1364–1367.
[48] S. Raeissi, L.J. Florusse, C.J. Peters, J. Chem. Eng. Data 56 (2011) 1105–1107.
[49] S. Raeissi, C.J. Peters, Fluid Phase Equilib. 294 (2010) 67–71.
[50] J. Kumełan, A. Pérez-SaladoKamps, D. Tuma, G. Maurer, Ind. Eng. Chem. Res. 46–24 (2007) 8236–8240.
[51] L.J. Florusse, S. Raeissi, C.J. Peters, J. Chem. Eng. Data 53 (2008) 1283–1285.
[52] M. Krummen, P. Wasserscheid, J. Gmehling, J. Chem. Eng. Data 47 (2002) 1411–1417.
[53] A. Heintz, D.V. Kulikov, S.P. Verevkin, J. Chem. Eng. Data 47 (2002) 894–899.
[54] A. Heintz, L.M. Casás, I.A. Nesterov, V.N. Emel'yanenko, S.P. Verevkin, J. Chem. Eng. Data 50 (2005) 1510–1514.
[55] A. Heintz, S.P. Verevkin, D. Ondo, J. Chem. Eng. Data 51 (2006) 434–437.
[56] T.M. Letcher, A. Marciniak, M. Marciniak, U. Domanska, J. Chem. Thermodyn. 37 (2005) 1327–1331.
[57] E.K. Shin, B.C. Lee, J.S. Lim, J. Supercrit, Fluids 45 (2008) 282–292.
[58] T.W. de Loos, Understanding phase diagrams, in: E. Kiran, J.M.H. Levelt Sengers (Eds.), Supercritical Fluids: Fundamentals for Application, Kluwer Academic Publishers, Dordrecht, 1994, pp. 65–89. NATO ASI Series, Series E: Applied Sciences.
[59] H. Renon, J.M. Prausnitz, Ind. Eng. Chem. Process Des. Dev. 7 (1968) 220–225.